Chinese Chemical Letters 37 (2026) 112031

Contents lists available at ScienceDirect

Chinese Chemical Letters

journal homepage: www.elsevier.com/locate/cclet

Polycation-based miRNA delivery system for choroidal neovascularization treatment

Qiannan Cao[a,b,1], Yu Liang[c,1], Weiyi Xia[c,1], Anna Guo[a,b,1], Mingxia Jiang[a,b], Lai Yang[d], Qiaoyan Dong[a,b], Wenming Zheng[a,b], Yingli Yao[a,b], Siting Zhang[a,b], Huilin Yuan[a,b], Pijun Su[a,b], Rongmei Zhou[c], Songyu Xu[c], Bo Chen[a,*], Jing Yao[c,e,*], Huapan Fang[a,b,*], Huayu Tian[a]

[a] College of Chemistry and Chemical Engineering, Innovation Laboratory for Sciences and Technologies of Energy Materials of Fujian Province (IKKEM), Department of Gastrointestinal Surgery, The First Affiliated Hospital of Xiamen University, Xiamen University, Xiamen 361005, China
[b] Shenzhen Research Institute of Xiamen University, Shenzhen 518000, China
[c] Eye Institute and Department of Ophthalmology, Eye & ENT Hospital, Fudan University, Shanghai 200031, China
[d] Department of Cardiology, Ezhou Hospital of Traditional Chinese Medicine, Ezhou 436000, China
[e] Department of Ophthalmology, The First Affiliated Hospital of Xinjiang Medical University, Urumqi 830013, China

ARTICLE INFO

Article history:
Received 24 August 2025
Revised 25 October 2025
Accepted 27 October 2025
Available online 28 October 2025

Keywords:
MicroRNA (miRNA)-based therapeutics
Polycationic nucleic acid carrier
Hydrophobic interactions
Disease progression
In vivo safety

ABSTRACT

MicroRNA (miRNA)-based therapeutics hold great promise for the treatment of ocular fundus diseases. However, naked miRNAs exhibit poor stability *in vivo*, are readily degraded by nucleases in body fluids, and their negative charge hinders efficient uptake by target cells. Therefore, a safe and effective nucleic acid delivery system is essential. In this study, we developed an efficient and safe polycationic nucleic acid carrier by modifying polyethyleneimine (PEI) with *p*-toluenesulfonyl chloride (*i.e.*, PEI-T_3). The introduction of tosyl groups onto PEI enhanced the hydrophobic interactions between polymer and cell membrane, and contributed to the cellular uptake of miRNA. Intravitreal injection of PEI-T_3/miRNA complexes caused negligible effects on retinal structure and function and did not induce neurotoxicity. Using microRNA-578 (miR-578) as the therapeutic gene, PEI-T_3/miR-578 treatment effectively downregulated the levels of vascular endothelial growth factor A (VEGF-A) and vascular cell adhesion molecule 1 (VCAM-1), suppressed the proliferation, migration, and tube formation of vascular endothelial cells. In a choroidal neovascularization (CNV) model, a single dose of PEI-T_3/miR-578 significantly relieved the disease progression and showed an excellent *in vivo* safety profile. This study provides a valuable reference for the *in vivo* delivery of miRNAs using polymeric carriers for the treatment of ocular fundus diseases.

© 2026 Published by Elsevier B.V. on behalf of Chinese Chemical Society and Institute of Materia Medica, Chinese Academy of Medical Sciences.

Age-related macular degeneration (AMD) is one of the leading causes of blindness in individuals over the age of 50 worldwide, with its prevalence steadily increasing with age [1,2]. Neovascular AMD (nAMD), a more aggressive subtype of AMD, is characterized by the abnormal formation of choroidal neovascularization (CNV), which leads to hemorrhage, edema, and other pathological changes that ultimately disrupt the retinal structure and function, resulting in irreversible vision loss. Currently, intravitreal injection of anti-vascular endothelial growth factor (VEGF) agents, such as Bevacizumab, Ranibizumab, and Aflibercept, remains the standard treatment for CNV. However, these agents fail to adequately address the multifactorial nature of AMD, leading to poor responsiveness in patients [3,4]. Moreover, frequent administration and the risk of adverse effects further limit their long-term clinical efficacy and patient compliance [5,6].

The anatomical accessibility of the eye and its immune-privileged status make nucleic acid-based therapeutics particularly well-suited for the treatment of retinal diseases. In recent years, oligonucleotides have gained increasing attention as therapeutic agents due to their small molecular size and high sequence specificity [7,8]. Among them, microRNAs (miRNAs), a class of endogenous non-coding RNAs, offer distinct advantages for targeting complicated diseases. They can simultaneously regulate multiple downstream genes at the post-transcriptional level, exhibit prolonged bioactivity, and evoke low immunogenicity [9]. A growing body of evidence suggests that miRNAs are involved in the pathogenesis of CNV, providing a broad array of molecular targets

* Corresponding authors.
E-mail addresses: chenbo7892@xmu.edu.cn (B. Chen), yaojingxiao@163.com (J. Yao), hpfang@xmu.edu.cn (H. Fang).
[1] These authors contributed equally to this work.

https://doi.org/10.1016/j.cclet.2025.112031
1001-8417/© 2026 Published by Elsevier B.V. on behalf of Chinese Chemical Society and Institute of Materia Medica, Chinese Academy of Medical Sciences.

for nucleic acid-based therapy [10,11]. miR-578 is a microRNA located on human chromosome 4 and predicted to form a canonical stem-loop precursor structure. Although still relatively understudied, emerging evidence suggests its involvement in the regulation of angiogenesis and related pathological processes. Notably, recent work has associated miR-578 with ocular neovascularization, particularly CNV. Dysregulation of miR-578 has been linked to aberrant expression of angiogenic factors, contributing to pathological vessel growth. Conversely, restoring its activity appears to suppress neovascularization, underscoring its potential as a novel therapeutic target for CNV [12]. However, the inherent instability, susceptibility to enzymatic degradation, and poor cellular uptake of miRNAs severely limit their *in vivo* applications, necessitating the development of safe and efficient delivery carriers.

Although viral carriers exhibit high transfection efficiency, their clinical use is hindered by immunogenicity, high production costs, and complex manufacturing procedure [13,14]. In contrast, nonviral delivery systems are more appealing for clinical translation due to their enhanced biosafety, abundant sources, and design flexibility [15–20]. Among them, polyethylenimine (PEI) is one of the most extensively used polymeric gene carriers [21–25]. For instance, PEI with molecular weight of 25,000 Daltons (PEI25k) exhibits high gene delivery efficiency and low immunogenicity, whereas its high positive charge density can lead to severe cytotoxicity, which limits its broader application [26–29]. Functionalizing PEI with specific chemical groups to introduce multiple interactions between the carrier and the cell membrane serves as an alternative strategy to enhance transfection efficiency and improve biocompatibility of carrier [22,30]. *p*-Toluenesulfonyl chloride (TsCl) contains both an electron-withdrawing sulfonyl group and a hydrophobic aromatic ring, making it particularly suitable for enhancing the stability and membrane affinity of cationic carriers. Incorporating *p*-toluenesulfonyl (tosyl) groups into PEI can increase polymer hydrophobicity, thereby strengthening nucleic acid complexation, promoting membrane interactions, and facilitating endosomal escape. The aromatic moiety may further stabilize polyplexes through π–π or hydrophobic stacking interactions, improving resistance to dissociation in serum. By controlling the degree of tosylation, the balance between transfection efficiency and cytotoxicity can be optimized for effective delivery, which remains a critical requirement for the development of effective delivery systems.

In this study, we modified PEI with TsCl (abbreviated as PEI-T_3) to introduce hydrophobic interactions between the polymeric carrier and the cell membrane. This modification significantly enhanced the cellular uptake efficiency of the PEI/miRNA complexes while maintaining excellent biocompatibility, thereby effectively resolving the dilemma between achieving high transfection efficiency and maintaining low cytotoxicity associated with polycation-based gene delivery systems. Herein, miR-578 was selected as the therapeutic gene, and treatment with PEI-T_3/miR-578 effectively suppressed the proliferation, migration, and tube formation of vascular endothelial cells, as well as downregulated the expression levels of VEGF-A and vascular cell adhesion molecule 1 (VCAM-1). In a mouse model of CNV, a single intravitreal injection of PEI-T_3/miR-578 significantly inhibited pathological vascular leakage and markedly delayed the progression of CNV. Moreover, no local or systemic toxicity was observed following administration of PEI-T_3/miR-578. This work provides valuable insight into the clinical application of miRNA-based therapies for ocular fundus diseases and demonstrates promising translational potential. miRNA-based technologies have been widely applied in the diagnosis and treatment of various diseases [31–33]. However, free miRNA sequences typically are negatively charged and unfavorable for uptake by target cells, thereby reducing the efficacy of miRNA therapeutics [34,35]. Therefore, it is necessary to develop efficient miRNA delivery carriers. Polymeric carriers have attracted increasing attention due to their low immunogenicity, abundant sources, and controllable structures. In this study, we synthesized *p*-toluenesulfonyl-modified polyethyleneimine (abbreviated as PEI-T) as a delivery carrier, introducing hydrophobic interactions between the carrier and the cell membrane to enhance miRNA delivery efficiency. As shown in Fig. S2 (Supporting information), PEI-T_3 containing different numbers of tosyl groups were prepared by reacting TsCl with polyethyleneimine at varying molar feed ratios (100:1, 200:1, 300:1, and 400:1). The successful synthesis of PEI-T was confirmed *via* hydrogen nuclear magnetic resonance (^{1}H NMR) spectra (Figs. S3–S6 in Supporting information), with tosyl grafting numbers of 91.2, 191.9, 276.9, and 331.2, respectively, and the resulting polymers were named PEI-T_1, PEI-T_2, PEI-T_3, and PEI-T_4 (Table S1 in Supporting information). In addition, GPC analysis showed that PEI-T_3 exhibited a number-average molecular weight (Mn) of 47,200, a weight-average molecular weight (Mw) of 66,500, and a polydispersity index (PDI) of 1.41 (Fig. S7 in Supporting information), indicating a relatively narrow molecular weight distribution.

Next, the *in vitro* biocompatibility of polymer/miRNA complexes at various mass ratios (20/1, 10/1, 5/1, 2.5/1, and 1/1) was evaluated in human umbilical vein endothelial cells (HUVECs) (Fig. S8 in Supporting information). Compared with PEI/miRNA complexes, all the PEI-T_n/miRNA ($n = 1$, 2, 3, and 4) exhibited significantly improved biocompatibility at same mass ratio of polymer/miRNA. Moreover, even at high mass ratios such as 20/1 and 10/1, PEI-T_n/miRNA-treated cells maintained a viability above 75%. Moreover, with the increasing number of tosyl group, the biocompatibility of PEI-T_n/miRNA complexes exhibited an upward trend. This was because tosyl modification consumed the primary amino groups of PEI, thereby reducing the surface positive charge density of carrier/miRNA, and ultimately effectively lowering the toxicity of the carrier/miRNA. Notably, PEI-T_4/miRNA complexes exhibited cell viability above 95% across all tested mass ratios. In addition, we found that PEI-T_3/miRNA exhibited excellent biocompatibility in both 293T and CHO normal cell lines, maintaining over 80% cell viability even at higher mass ratios (Figs. S9 and S10 in Supporting information). These results demonstrated that PEI-T_n possessed the excellent biocompatibility.

To further evaluate the cellular uptake efficiency of polymeric carriers loaded with miRNA, Cy5-labeled non-functional miRNA was used as a reporter and the uptake efficiency of PEI-T_n/miRNA was measured in HUVECs by flow cytometry. As shown in Fig. 1A, all PEI-T_n/miRNA complexes showed superior cellular uptake efficiency compared to PEI/miRNA at the same mass ratios. This phenomenon was primarily attributed to the incorporation of tosyl groups, which strengthened hydrophobic interactions between the delivery carrier and the cell membrane, thus promoting cellular internalization [36,37]. Interestingly, as the grafting number of tosyl group increased, the cellular uptake efficiency of PEI-T_n/miRNA complexes first increased and then decreased, and PEI-T_3/miRNA exhibited the optimal cellular uptake efficiency at mass ratio of 5/1. This phenomenon was attributed that the introduction of tosyl groups onto PEI enhanced hydrophobic interactions between polymer and cell membrane while simultaneously depleting amino groups on PEI, and leaded to a reduction in electrostatic interactions with the cell membrane. Moreover. the confocal imaging results clearly demonstrated that PEI-T_3/miRNA exhibited efficient cellular uptake compared to PEI/miRNA (Fig. 1B and Fig. S11 in Supporting information). Furthermore, quantitative flow cytometry analysis confirmed that PEI-T_3/miRNA complexes efficiently mediated the intracellular delivery of miRNA into HUVECs, resulting in a significantly enhanced uptake compared with PEI/miRNA or naked miRNA controls (Fig. S12 in Supporting information). Given that PEI-T_3/miRNA achieved the highest cellular uptake performance at

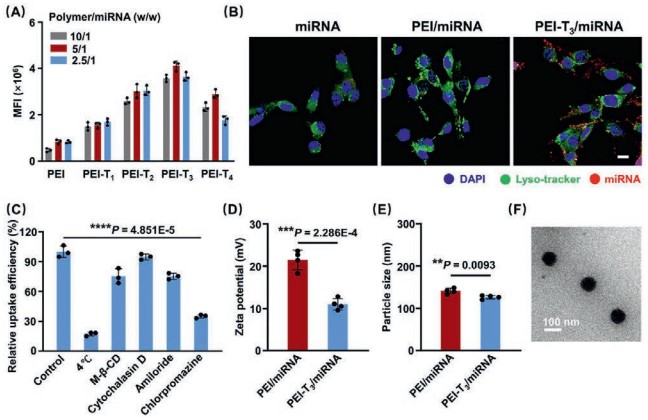


Fig. 1. Construction and characterization of polycation-based miRNA delivery systems. (A) Mean fluorescence intensity (MFI) of HUVECs incubated with PEI-T_n/miRNA and PEI/miRNA at various mass ratios. (B) Representative cellular uptake images of PEI-T_3/miRNA, PEI/miRNA, and miRNA in HUVECs, scale bar: 10 μm. (C) Relative uptake efficiency of PEI-T_3/miRNA in HUVECs preincubated with endocytosis inhibitors. (D) Particle size and (E) zeta potential of PEI-T_3/miRNA and PEI/miRNA. (F) Representative TEM image of PEI-T_3/miRNA. Scale bar: 100 nm. Data are presented as the mean ± SD ($n = 3$ independent samples in A and C; $n = 4$ independent samples in D and E). *P* values are obtained by the two-tailed Student's *t*-test. $^{**}P < 0.01$, $^{***}P < 0.001$, $^{****}P < 0.0001$. A representative image of four independent samples from each group is shown in B and F.

a mass ratio of 5/1, this mass ratio was selected for subsequent experiments.

To further elucidate the cellular uptake mechanism of the PEI-T_3/miRNA complexes, HUVECs were pretreated with different endocytosis inhibitors, including methyl-β-cyclodextrin (M-β-CD, caveolae-mediated endocytosis), cytochalasin D (actin-dependent endocytosis), and amiloride (macropinocytosis-mediated endocytosis), and chlorpromazine (clathrin-mediated endocytosis). As shown in Fig. 1C, it was observed that the cellular uptake efficiency of PEI-T_3/miRNA was markedly decreased when the cells were cultured at 4 °C, indicating that uptake mechanism of PEI-T_3/miRNA complexes was energy-dependent [38]. Furthermore, we found that chlorpromazine treatment markedly reduced the uptake efficiency of PEI-T_3/miRNA, suggesting that PEI-T_3/miRNA entered target cells *via* clathrin-mediated endocytosis pathway (Fig. 1C).

Physicochemical properties of polymeric carriers had a significant impact on their delivery efficiency [39]. Therefore, we further evaluated the particle size and zeta potential of the PEI-T_3/miRNA complexes. As expected, PEI-T_3/miRNA showed lower zeta potential than PEI/miRNA at the same mass ratio (Fig. 1D). This was mainly because the introduction of the p-toluenesulfonyl group consumed primary amine groups of PEI backbone, thereby reducing the positive charge density on the surface of the carrier/miRNA complexes. In addition, the hydrodynamic size results showed that PEI-T_3/miRNA complexes possessed a smaller particle size than PEI/miRNA complexes, measuring 126.4 ± 4.3 and 140.4 ± 6.4 nm, respectively (Fig. 1E). In general, polycationic carriers with more positive charges were more favorable of compressing nucleic acid into smaller nanoparticles. Nevertheless, the size data of PEI/miRNA and PEI-T_3/miRNA were the opposite. This phenomenon was primarily due to the fact that introduction of tosyl groups promoted the formation of hydrophobic interactions between PEI-T_3 and the bases of nucleic acid, thereby facilitating the compression of miRNA. Transmission electron microscopy (TEM) images showed that PEI-T_3/miRNA complexes were uniform spherical nanoparticles with a size of approximately 93.1 ± 1.7 nm (Fig. 1F). Furthermore, it was found that PEI-T_3/miRNA exhibited an excellent stability in both zeta potential and particle size (Figs. S13 and S14 in Supporting information). In addition, the ability of PEI-T_3 to encapsulate miRNA was evaluated by agarose gel electrophoresis. In the PEI-T_3 group, the migration of miRNA bands was almost completely retarded, indicating that the carrier PEI-T_3 was able to efficiently load miRNA and thereby protect it from degradation (Fig. S15 in Supporting information). Collectively, these results suggested that PEI-T_3/miRNA nanocomplexes possessed good biocompatibility and excellent *in vitro* delivery performance, making them an ideal candidate for gene-based therapeutics for ocular diseases.

Recent studies have shown that ocular fundus neovascular diseases were closely associated with endogenous miRNA, specifically miR-578 [12,40]. In the lesion tissues of laser-induced CNV, the overexpressed circular RNA-ZBTB44 acted as miR-578 sponge to down-regulate levels of miR-578 and subsequently increase VEGF-A expression, consequently accelerating the disease progression. In this study, to evaluate the therapeutic efficacy of this miRNA delivery system, miR-578 was selected as therapeutic gene. Firstly, we evaluated the levels of VEGF-A in HUVECs after treatment with the PEI-T_3/miR-578 complexes by real-time quantitative polymerase chain reaction (RT-qPCR) technique, and PEI/miR-578 was served as control. As shown in Fig. S16 (Supporting information), compared to the untreated group, the free miR-578 hardly downregulated VEGF-A levels in HUVECs. The phenomenon should be attributed to the poor cellular uptake efficiency of free miR-578 (Fig. 1B), which consequently limited the efficacy of miR-578. In addition, the VEGF-A levels of HUVECs were moderately inhibited in the PEI/miR-578 group. Notably, the inhibitory effect on VEGF-A was most pronounced in the PEI-T_3/miR-578 group. This was because PEI-T_3 could efficiently promote the cellular uptake of miR-578, thereby enhancing its regulation of VEGF-A in HUVECs.

Recent studies have reported that vascular cell adhesion molecule-1 (VCAM-1) played an important role in exacerbating ocular fundus neovascular diseases [41–43], and it has also been shown that miR-578 could significantly downregulate VCAM-1 expression [12]. Therefore, we further evaluated the levels of VCAM-1 in HUVECs following treatment with PEI-T_3/miR-578. As expected, the free miR-578 group exhibited a poor inhibitory effect on VCAM-1 and the PEI/miR-578 treatment showed a moderate suppression of VCAM-1. In contrast, PEI-T_3/miR-578 significantly downregulated VCAM-1 levels in HUVECs (Fig. S17 in Supporting information). In addition, we further evaluated the proliferation of HUVECs before and after incubation with PEI-T_3/miR-578 by the 5-ethynyl-2′-deoxyuridine (EdU) incorporation assay. It was observed that PEI-T_3/miR-578 incubation significantly inhibited HUVEC proliferation, whereas free miR-578 and PEI/miR-578 exhibited minor effects on cell proliferation (Figs. 2A and B).

Moreover, we further evaluated the tube formation ability of HUVECs after different treatments. Compared with the untreated group, the total tube length in the free miR-578 group showed negligible changes (Figs. 2C and D). The PEI/miR-578 group exhibited a moderate reduction in total tube length. Among all groups, the PEI-T_3/miR-578 group displayed the lowest total tube length and the lowest network complexity, indicating that PEI-T_3/miR-578 treatment effectively inhibited tube formation in HUVECs and demonstrated excellent anti-angiogenic activity. In addition, the Transwell assay was performed to further evaluate the migration efficiency of HUVECs receiving different treatments. It was showed that PEI-T_3/miR-578 treatment effectively inhibited HUVEC migration (Figs. 2E and F). Collectively, these results clearly demonstrated that PEI-T_3/miR-578 could efficiently downregulate VEGF-A and VCAM-1 expression, thereby suppressing cell proliferation, tube formation, and migration, ultimately exhibiting outstanding *in vitro* anti-angiogenic properties.

Based on the above results, it was concluded that PEI-T_3/miR-578 could significantly inhibit *in vitro* angiogenesis by downreg-

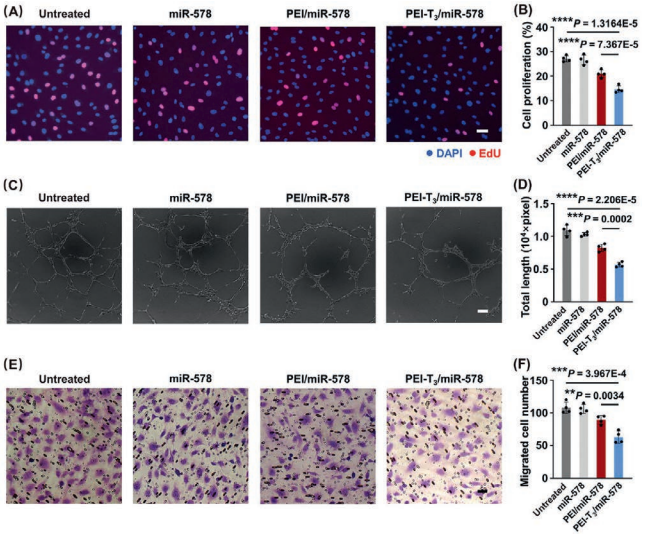


Fig. 2. PEI-T_3/miR-578 exhibited highly efficient anti-angiogenic activity *in vitro*. (A) Representative cell proliferation images and (B) corresponding cell proliferation percentages of HUVECs incubated with PEI-T_3/miR-578, PEI/miR-578, or miR-578. (C) Representative tube formation images and (D) total tube length of HUVECs incubated with PEI-T_3/miR-578, PEI/miR-578, or miR-578 in the tube formation assay. (E) Representative cell migration images and (F) corresponding migrated cell number of HUVECs incubated with PEI-T_3/miR-578, PEI/miR-578, or miR-578 in Transwell assay. Scale bar: 100 μm. Data are presented as the mean ± SD ($n = 4$ independent samples in B, D, and F). *P* values are obtained by the two-tailed Student's *t*-test. $^{**}P < 0.01$, $^{***}P < 0.001$, $^{****}P < 0.0001$. A representative image of four independent samples from each group is shown in A, C and E.

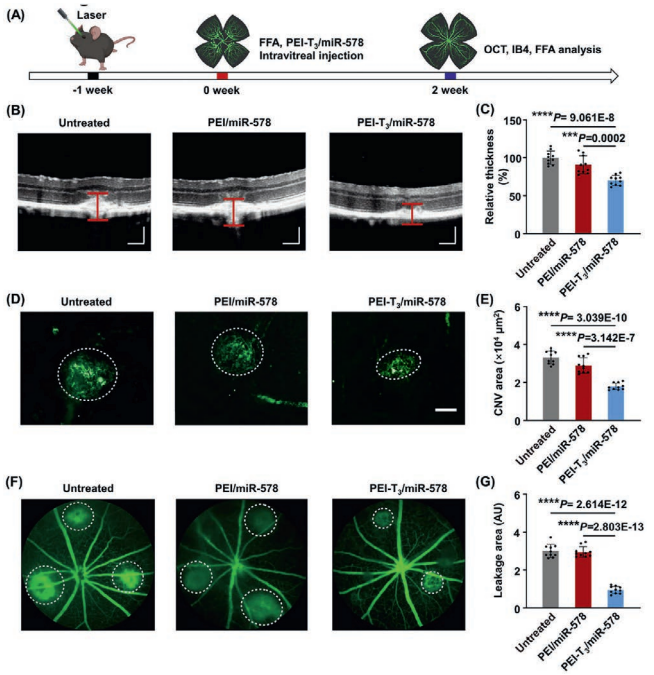


Fig. 3. PEI-T_3/miR-578 significantly alleviated the progression of CNV. (A) Schematic illustration of the treatment of laser-induced CNV in mice. (B) Representative OCT images and (C) relative retinal thickness of CNV-bearing mice receiving different treatments. Scale bar: 150 μm. (D) Representative Isolectin GS-IB4 fluorescence images to evaluate the CNV area and (E) corresponding CNV area in mice receiving different treatments. Scale bar: 100 μm. (F) Representative fundus fluorescein angiography (FFA) images and (G) corresponding leakage area of CNV-bearing mice receiving different treatments. Data are presented as the mean ± SD ($n = 10$ independent samples in C, E, and G). *P* values are obtained by the two-tailed Student's *t*-test. $^{***}P < 0.001$, $^{****}P < 0.0001$. A representative image of ten independent samples from each group is shown in B, D and F.

ulating the expression of VEGF-A and VCAM-1. To further evaluate the therapeutic efficacy of PEI-T_3/miR-578 against ocular neovascular diseases, a laser-induced CNV model was established. One week after model induction, intravitreal administration of PEI-T_3/miR-578 was performed at a miR-578 dose of 0.2 μg per mouse, and therapeutic outcomes were assessed after two weeks (Fig. 3A). As shown in Figs. 3B and C, optical coherence tomography (OCT) imaging showed that, compared with the untreated group, mice treated with PEI/miR-578 exhibited negligible changes in choroidal thickness. In contrast, mice treated with PEI-T_3/miR-578 displayed a marked reduction in choroidal thickness, indicating that PEI-T_3/miR-578 effectively alleviated CNV-associated swelling.

Moreover, we further employed griffonia simplicifolia isolectin B4 (Isolectin GS-IB4) fluorescence staining to evaluate the area of CNV in mice receiving different treatments. The CNV area in the PEI/miR-578 group showed negligible reduction, whereas PEI-T_3/miR-578 treatment reduced the CNV area to 53.9% ± 5.4% of the untreated group (Figs. 3D and E). In addition, fluorescein fundus angiography was conducted to evaluate vascular leakage in the choroid. The vascular leakage area in the PEI/miR-578 group was only negligibly reduced compared with the untreated group. Notably, PEI-T_3/miR-578 treatment significantly decreased vascular leakage to 31.6% ± 6.3% of the untreated level (Figs. 3F and G). In addition, immunofluorescence analysis demonstrated that treatment with PEI-T/miR-578 markedly reduced the expression of VEGF-A and VCAM-1 within the CNV lesion area compared with the control group, indicating that PEI-T/miR-578 effectively suppresses angiogenic signaling in CNV lesions (Figs. S18 and S19 in Supporting information). Collectively, these results suggested that PEI-T_3/miR-578 treatment effectively suppressed neovascularization and reduced vascular leakage in the CNV model, thereby markedly alleviating disease progression. After evaluating the therapeutic efficacy of PEI-T_3/miR-578 nanoparticles in the CNV model, we next investigated the *in vivo* safety profile. All animal tests followed the guidelines set by the Animal Ethics and Use Committee of Xiamen University.

CRediT authorship contribution statement

Qiannan Cao: Writing – original draft, Methodology, Investigation, Formal analysis, Data curation. **Yu Liang:** Writing – original draft, Methodology, Investigation, Formal analysis, Data curation. **Weiyi Xia:** Methodology, Investigation, Formal analysis, Data curation. **Anna Guo:** Methodology, Investigation, Formal analysis, Data curation. **Mingxia Jiang:** Formal analysis, Data curation. **Lai Yang:** Writing – review & editing, Methodology, Formal analysis. **Qiaoyan Dong:** Methodology, Data curation. **Wenming Zheng:** Writing – review & editing, Data curation. **Yingli Yao:** Writing – review & editing, Data curation. **Siting Zhang:** Writing – review & editing, Data curation. **Huilin Yuan:** Writing – review & editing, Data curation. **Pijun Su:** Writing – review & editing, Formal analysis. **Rongmei Zhou:** Writing – review & editing, Formal analysis. **Songyu Xu:** Writing – review & editing, Formal analysis. **Bo Chen:** Writing – review & editing, Writing – original draft, Investigation, Formal analysis, Data curation. **Jing Yao:** Writing – review & editing, Writing – original draft, Formal analysis, Data curation. **Huapan Fang:** Writing – review & editing, Writing – original draft, Methodology, Funding acquisition, Formal analysis, Data curation, Conceptualization. **Huayu Tian:** Writing – review & editing, Funding acquisition.

Declaration of competing interest

The authors declare that they have no known competing financial interests or personal relationships that could have appeared to influence the work reported in this paper.

Acknowledgments

This work was acknowledged to Natural Science Foundation of Xiamen, China (No. 3502Z202371004); Shenzhen Science and Technology Program (No. JCYJ20240813145515020); National Natural Science Foundation of China (Nos. 52473150, 52433006, 52495010, 52203183, 51925305, 82460209, 82301217); Fundamental Research Funds for the Central Universities (No. 20720230004); National Key Research and Development Program of China (No. 2021YFB3800900); Xiamen Medical and Health Guidance Project (No. 3502Z20209017) and the Talent Cultivation Project Funds for the Innovation Laboratory for Sciences and Technologies of Energy Materials of Fujian Province (No. HRTP-[2022]52).

Supplementary materials

Supplementary material associated with this article can be found, in the online version, at doi:10.1016/j.cclet.2025.112031.

References

[1] R.S. Apte, C.G. Solomon, N. Engl. J. Med. 385 (2021) 539–547.
[2] P. Mitchell, G. Liew, B. Gopinath, T.Y. Wong, Lancet 392 (2018) 1147–1159.
[3] W.M. Amoaku, U. Chakravarthy, R. Gale, et al., Eye 29 (2015) 721–731.
[4] I.U. Scott, P.C. VanVeldhuisen, M.S. Ip, et al., J. Am. Med. Assoc. 317 (2017) 2072–2087.
[5] J.A. Wells, A.R. Glassman, A.R. Ayala, et al., N. Engl. J. Med. 372 (2015) 1193–1203.
[6] N. Rayess, E. Rahimy, P. Storey, et al., Am. J. Ophthalmol. 165 (2016) 88–93.
[7] S. Wang, D. Weissman, Y. Dong, Nat. Rev. Drug Discov. 24 (2025) 828–851.
[8] Q. Tang, A. Khvorova, Nat. Rev. Drug Discov. 23 (2024) 341–364.
[9] A. Mehta, D. Baltimore, Nat. Rev. Immunol. 16 (2016) 279–294.
[10] D.W. Penga, C.L. Lana, L.Q. Donga, et al., Proc. Natl. Acad. Sci. U. S. A. 119 (2022) e2204795119.
[11] C.H. Liu, Y. Sun, J. Li, et al., Pro. Natl. Acad. Sci. U. S. A. 112 (2015) 12163–12168.
[12] R.m. Zhou, L.j. Shi, K. Shan, et al., Theranostics 10 (2020) 3293–3307.
[13] J.B. Ulmer, U. Valley, R. Rappuoli, Nat. Biotechnology 24 (2006) 1377–1383.
[14] M.S. Gebre, L.A. Brito, L.H. Tostanoski, et al., Cell 184 (2021) 1589–1603.
[15] K.A. Hajj, K.A. Whitehead, Nat. Rev. Mater. 2 (2017) 17056.
[16] H. Fang, Y. Feng, J. Chen, H. Tian, X. Chen, Mater. Today Chem. 11 (2019) 269–282.
[17] H. Fang, Z. Guo, L. Lin, et al., J. Am. Chem. Soc. 30 (2018) 11992–12000.
[18] H. Zhang, X. You, X. Wang, et al., Proc. Natl. Acad. Sci. U. S. A. 118 (2021) e2005191118.
[19] Y. Sui, X. Hou, J. Zhang, et al., J. Mater. Chem. B 13 (2025) 10085–10117.
[20] H. Xu, J. Fan, J. Liu, et al., Chin. Chem. Lett. 36 (2025) 110833.
[21] X.Y. Guo, Z.Y. Yang, H.P. Fang, et al., Chin. J. Polym. Sci. 42 (2024) 1699–1709.
[22] H. Fang, L. Lin, J. Chen, et al., Biomater. Sci. 7 (2019) 1716–1728.
[23] D. Xie, Q. Cao, H. Fang, Y. Li, H. Tian, Chin. Chem. Lett. 37 (2026) 111032.
[24] T. Nie, Z. He, J. Zhu, L. Liu, Y. Chen, Adv. Ther. 3 (2020) 2000016.
[25] T. Nie, Z. He, Y. Zhou, et al., ACS Appl. Mater. Interfaces 11 (2019) 29593–29603.
[26] S. Zhang, H. Fang, H. Tian, Biomacromolecules 25 (2024) 7015–7057.
[27] M. Jiang, H. Fang, H. Tian, J. Control. Release 380 (2025) 138–174.
[28] W. Xiao, F. Wang, Y. Gu, et al., Chin. Chem. Lett. 35 (2024) 108755.
[29] S. Ding, E. Alexander, H. Liang, et al., Chem. Rev. 125 (2025) 4009–4068.
[30] H. Fang, Z. Guo, J. Chen, et al., Nat. Commun. 12 (2021) 6742.
[31] R. Rupaimoole, F.J. Slack, Nat. Rev. Drug Discov. 16 (2017) 203–222.
[32] J.K. Cheong, Y.C. Tang, L. Zhou, H. Cheng, H.P. Too, Curr. Opin. Biotechnol. 74 (2022) 256–262.
[33] Z. Fang, X. Zhang, H. Huang, J. Wu, Chin. Chem. Lett. 33 (2022) 1693–1704.
[34] C. Diener, A. Keller, E. Meese, Trends Genet. 38 (2022) 613–626.
[35] A. Jeyaram, T.N. Lamichhane, S. Wang, et al., Mol. Ther. 28 (2020) 975–985.
[36] S. Dong, H. Fang, J. Zhu, et al., ACS Nano 19 (2025) 2742–2758.
[37] H. Fang, Y. Wu, L. Chen, et al., ACS Nano 17 (2023) 4748–4763.
[38] D. Jana, Z. Han, X. Huang, et al., ACS Nano 18 (2024) 16674–16683.
[39] R. De, M.K. Mahata, K.T. Kim, Adv. Sci. 9 (2022) 2105373.
[40] J. Song, Y.K. Kim, Mol. Ther. Nucl. Acids 24 (2021) 284–293.
[41] M. Shyam, S. Sidharth, A. Veronica, et al., Mol. Biol. Rep. 52 (2025) 380.
[42] Y. Liu, J. Shen, S.D. Fortmann, J. Wang, D. Vestweber, P.A. Campochiaro, JCI Insight 2 (2017) e95530.
[43] W. Deng, C. Yi, W. Pan, et al., Immunity Ageing 20 (2023) 65.